JOURNAL OF Applied Polymer SCIENCE

Property reinforcement of acrylonitrile-butadiene-styrene by simultaneous incorporation of carbon nanotubes and self-prepared copper particles

Gen Lin Wang,[1,2] Lei Duan,[1] Ke Hong Ding,[2] Ming Zhang[1]
[1]College of Chemistry and Chemical Engineering, Yangzhou University, Yangzhou 225002, China
[2]Jiangsu Yangnong Chemical Group Co., Ltd, Yangzhou 225002, China
Correspondence to: M. Zhang (E-mail: lxyzhangm@yzu.edu.cn)

ABSTRACT: In this article, copper (Cu) crystallites were successfully prepared via low temperature molten salt method, and the possible formation mechanisms were proposed. The conductive fillers of multiwalled carbon nanotubes (MWCNTs) and as-prepared Cu particles were designed and introduced into acrylonitrile-butadiene-styrene (ABS) blend to prepare different conductive composites. The dispersion states of conductive fillers and the morphologies of the composites were characterized using a field emission scanning electron microscope. The electrical resistivity of different composites was measured. The results showed that Cu and MWCNTs exhibited a synergistic effect in decreasing the electrical resistivity of the Cu/MWCNTs/ABS composites, because Cu that could locate between MWCNTs chain segments provides a better charge transport in the conductive pathways. Compared with pure ABS, the tensile strength, elastic modulus and thermal stability of the Cu/MWCNTs/ABS composites were significantly improved with the incorporation of Cu and MWCNTs. © 2014 Wiley Periodicals, Inc. J. Appl. Polym. Sci. **2015**, *132*, 41738.

KEYWORDS: composites; conducting polymers; mechanical properties; thermal properties

Received 9 August 2014; accepted 11 November 2014
DOI: 10.1002/app.41738

INTRODUCTION

Copper particles (Cu) are widely used in the industry to achieve the conductive and wear-resisting polymer composites due to its low cost and abundant supply. Various techniques have been devoted to synthesize copper particles,[1–10] including chemical reduction, thermal reduction, microemulsion techniques, laser ablation, vacuum vapor deposition, irradiation methods, solid-state methods, and the polyol process. Among these methods, the polyol method is fortunately allowed to prepare copper particles in air atmosphere rather than oxygen-free atmosphere. In addition, the polyol itself acts as a reducing agent and complexation for copper particles preparation. Ramyadevi *et al.*[5] reported the synthesis of copper nanoparticles using a modified polyol (ethylene glycol) method by the reduction of copper acetate hydrate in the presence of Tween 80 by refluxing between 190 and 200°C. Chiang *et al.*[11] indicated that the copper particles were successfully deposited on bamboo charcoal by a polyol process using copper acetate as a precursor and ethylene glycol as both solvent and reducing agent. Sun *et al.*[12] synthesized the ultrafine copper particle in ethylene glycol in which sodium hydroxide was added. Generally, low molecular weight polyol such as ethylene glycol was oxidized at high temperature to form acetaldehyde that could reduce copper compound to copper particles.

It is well-known that acrylonitrile butadiene styrene (ABS) has been one of the most important polymers in various industrial fields due to its rigidity and chemical stability. However, ABS should have good electrical conductivity to avoid electrical failure caused by accumulation of electrostatic charges or to be used as an electric or electronic material. Addition of conductive fillers such as copper particles is the most efficient way to achieve the conductive composites.[13–16] However, high content of Cu must be required to fabricate the conductive polymer composites.[17] In other words, the percolation threshold of Cu is relatively large, which may be unfavorable for keeping and/or improving of other properties like strength and ductility. Multiwalled carbon nanotubes (MWCNTs) are considered as a versatile conductive filler in the polymer composite industry due to its large aspect ratio, good intrinsic electrical conductivity and excellent chemical properties.[18–21]

In this case, the electrical conductivity increases by orders of magnitude at the percolation threshold with increasing filler content, which depends on the dispersion state and the geometry of the filler. The higher electrical conductivity can be achieved with significantly lower MWCNTs content.[14,20,21]

Table I. The Relational Informations of the Synthesis and Characterization of the Cu/Mwcnts/Abs and MWCNTs/ABS Composites

	Composition (wt %)		TGA and DTG analyze	
Samples	Copper	MWCNTs	The maximum mass loss rate/(wt %/min)	The temperature of maximum mass loss rate/°C
S1	0	0	19.59	414.4
S2	10	0	13.39	414.2
S3	10	1	14.24	415.7
S4	10	3	14.41	417.8
S5	10	5	13.98	417.5
S6	10	7	14.55	421.6
S7	0	1	16.70	414.4
S8	0	3	18.06	421.0
S9	0	5	20.07	419.7
S10	0	7	18.57	421.4

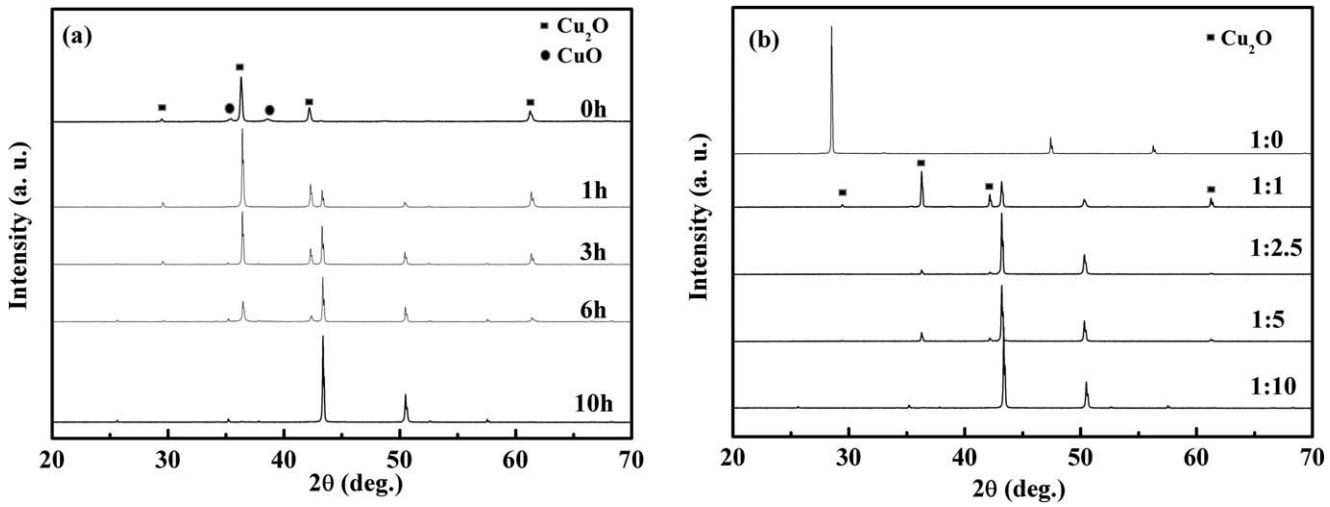

Figure 1. XRD patterns of the reduction of $CuCl_2 \cdot 2H_2O$ under (a) the different reaction time, (b) the different weight ratio of $CuCl_2 \cdot 2H_2O$ and the mixture of eutectic NaOH–KOH.

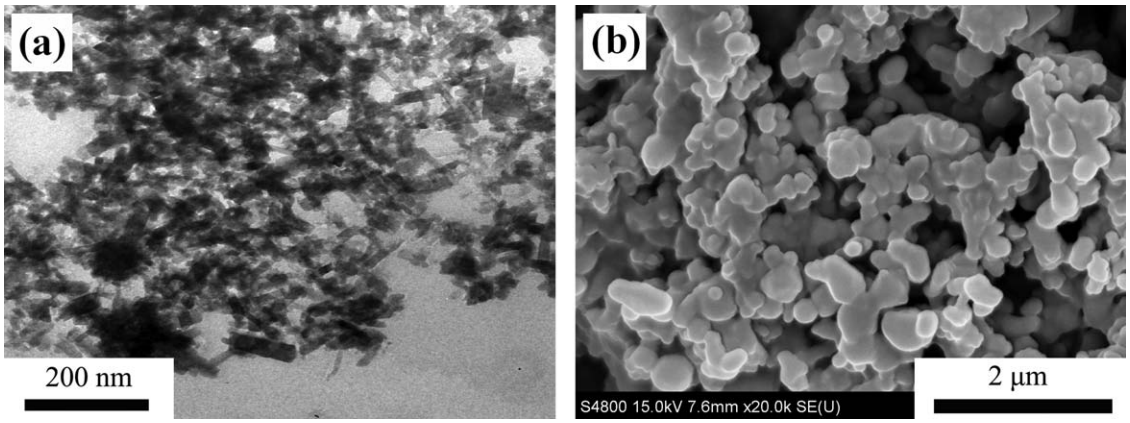

Figure 2. (a) TEM picture of CuCl and (b) FESEM picture of Cu powders by different routes.

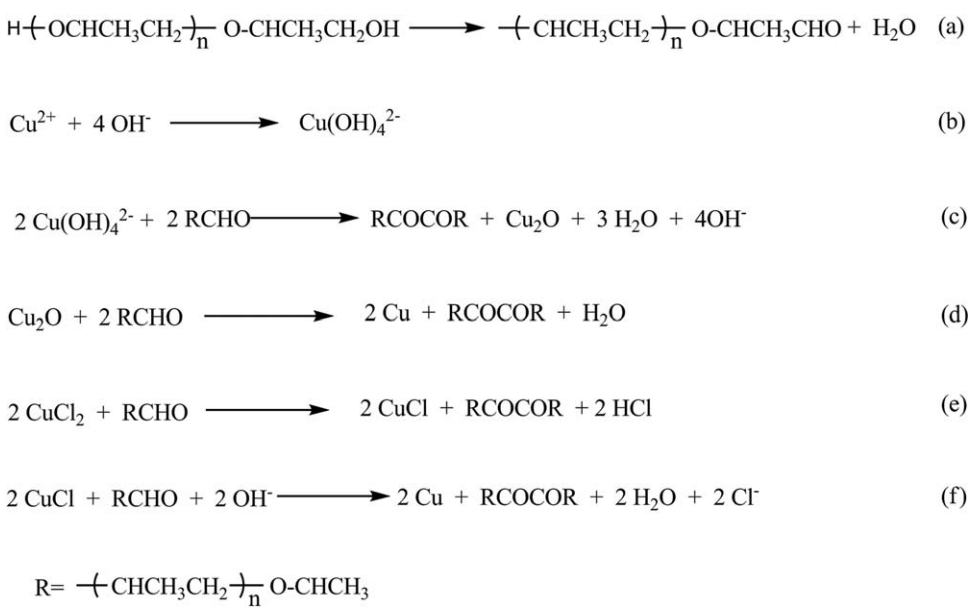

Figure 3. The equations of preparation of Cu crystallites by low temperature molten salt method.

However, the thermal stability of composites can be decreased because the external heat is easily transferred to polymer matrix by the MWCNTs network layer. It is serious that accelerates the melt and decomposition of internal polymer. Fortunately, the copper has very high thermal conductivity and specific heat capacity, e.g., 401 W/mK at 25°C, 400 W/mK at 125°C, and 398 W/mK at 225°C,[11] which locates between MWCNTs chain segments, and it also provides a better charge and thermal transport and storage in the conductive pathways. Consequently, the thermal stability of Cu/MWCNTs/ABS composites can be increased due to the excellent synergistic effect of Cu particles and MWCNTs.

Based on the above discussion, the major aim of this study is to design and investigate the effect of the synergistic system consisted of Cu and MWNTs, on the mechanical, electrical resistivity and thermal properties of Cu/MWCNTs/ABS composites. Meanwhile, the copper particles were simply prepared using polymer-assisted low temperature molten salt method by the reduction of cupric chloride dihydrate. The reducing and complexation agent is the high molecular weight polypropylene glycol (PPG-400, molecular weight is 400). The molten salt system, namely NaOH-KOH (49.2 : 50.8 mol % ratio; melting point 170°C)[22] has been also exploited to catalyze alcohol into aldehyde.

EXPERIMENTAL

Materials

All the chemical reagents used in our experiments are of analytical grade. ABS (121H) was purchased from Ningbo Lejin Yongxin Chemical. MWCNTs (FloTube 9000) were supplied from

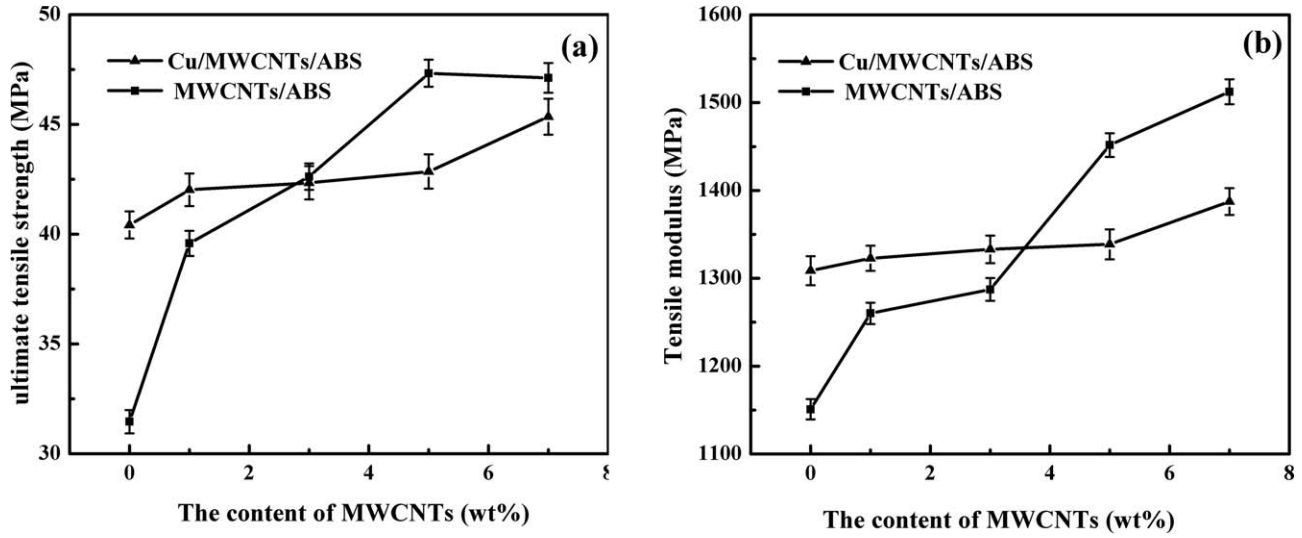

Figure 4. (a) The ultimate tensile strength and (b) the elastic modulus of Cu/MWCNTs/ABS, and MWCNTs/ABS composites (S1–S10) plotted versus the filler content.

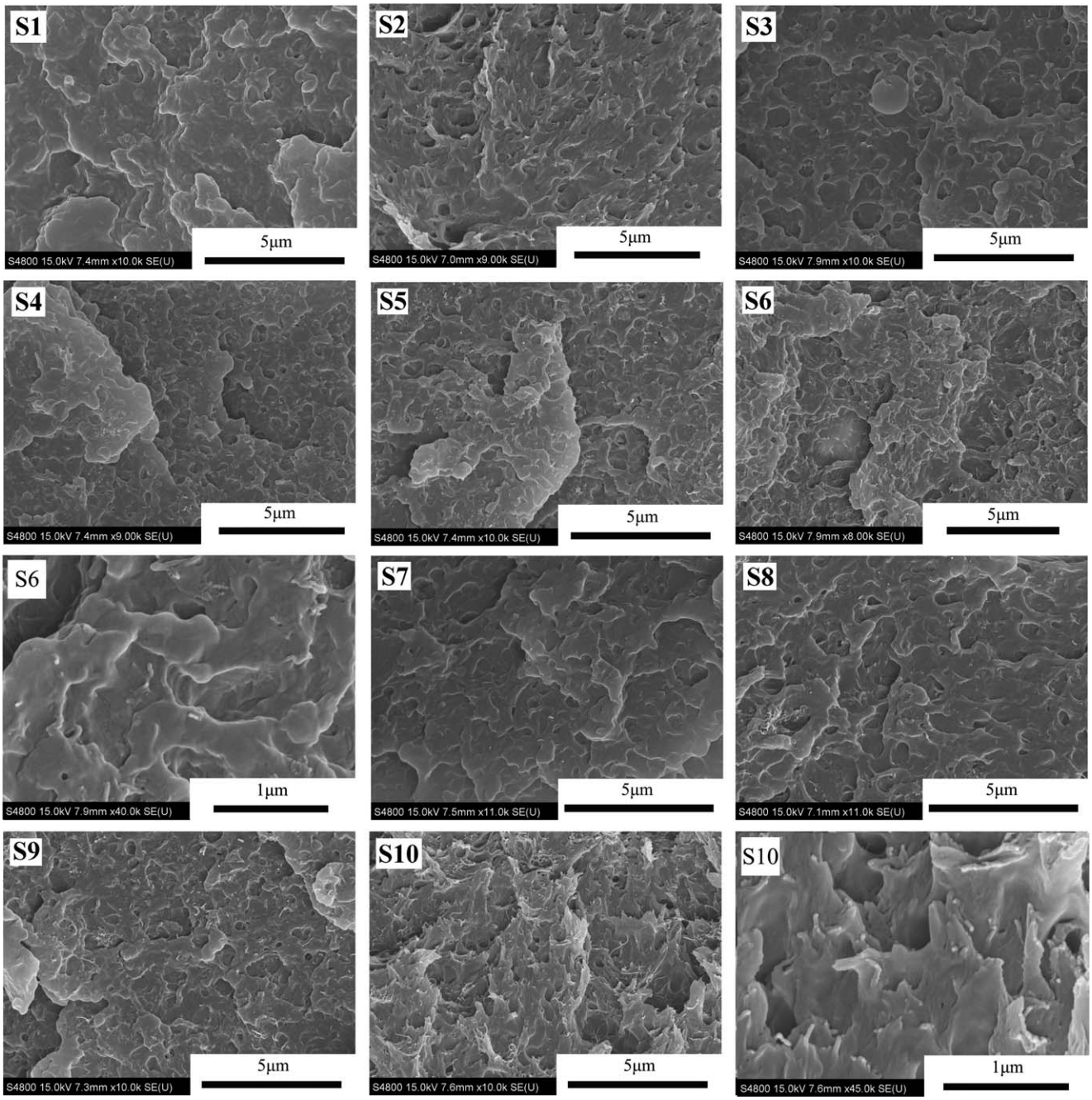

Figure 5. FESEM micrographs of the fracture surfaces of the Cu/MWCNTs/ABS and MWCNTs/ABS composites (S1–S10) with different magnification.

CNano Technology. The average diameter and length of the CNTs used is about 11 nm and 10 μm, respectively and the purity is above 95%. PPG-400 was obtained from Jiangsu Haian Petrochemical Plant Co. $CuCl_2{\cdot}2H_2O$, NaOH and KOH were Purchased from Sinopharm Chemical Reagent.

Preparation of Cu Particles via Molten Salt Method

1.0229 g $CuCl_2{\cdot}2H_2O$ and 10.2290 g of equimolar NaOH and KOH were ground evenly in a carnelian mortar, then mixed homogeneously with 8.1832 g PPG-400 and transferred to a corundum crucible. The crucible was heated in air at 180°C for 10 h. The temperature increase of 2°C every minute was used before the temperature reached 180°C. And after the thermal treatment, it was allowed to cool to room temperature naturally. The resultant products were washed carefully with distilled water and absolute alcohol to remove the alkali and organics, such as NaOH, KOH, and PPG-400. Finally, kermesinus copper particles were obtained and presented in nitrogen condition to prevent oxidation.

Preparation of Cu/MWCNTs/ABS and MWCNTs/ABS Composites

In order to facilitate the description, the designation and formulations of the samples are listed in Table I. Take the S3

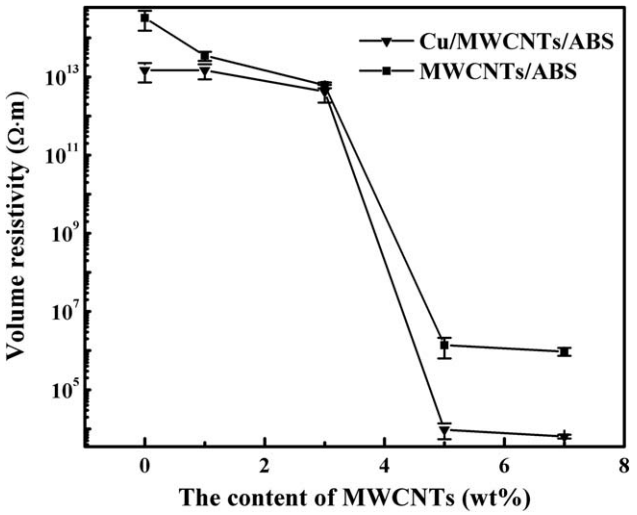

Figure 6. Variations of the electric resistivity of Cu/MWCNTs/ABS and MWCNTs/ABS composites (S1–S10).

(Table I) for example, Composites of Cu/MWCNTs/ABS (in which the weight ratio of Cu particles, MWCNTs and ABS was 10/1/100) were prepared by direct melt compounding in a HAAKE torque rheometer (R600, Thermo Fisher Scientific) at 200°C for 5 min. Specimens for mechanical and electrical measurements were compression molded at 200°C for 5 min under a pressure of 10 MPa (QLB-25T, Xizhang Xinhua Xiangsu machine).

Characterization of the Products

Powder XRD patterns of the obtained products were recorded at a scanning rate of 8°/min in the 2θ range of 20°–70°, using a Bruker D8 ADVANCE diffractometer system with a Cu-Kα irradiation ($\lambda = 1.5418$ Å). TEM images were taken with a Philips Tecnai12 transmission electron microscopy at an accelerating voltage of 120.0 kV. Field emission scanning electron microscope (FESEM) images analysis were carried out on a Japan Hitachi S-4800 FESEM (15 kV). Tensile testing was carried out on dumbbell-shaped samples (ISO 527/2) using a universal testing machine (Inston-3360, Instron). Thermal gravimetric analysis (TGA) was carried out using a thermal gravimetric analyzer (Pyris 1 TGA, PerkinElmer) at a heating rate of 10°C/min under nitrogen condition. The Digital High Resistance Test Fixture ZC36 (Shanghai 6th Electricity Meter) was applied to testing the electrical resistivity of the samples. Before measurement, all the samples were cleaned by ethyl alcohol to avoid the influence of the dust on the surface of samples.

RESULTS AND DISCUSSION

The reaction time and alkalinity of the reduction reaction play greatly important factors in the purity of copper particles, as shown in Figure 1. Figure 1(a) shows the XRD patterns of the products prepared by the reaction of $CuCl_2{\cdot}2H_2O$, eutectic NaOH-KOH and PPG-400 (1 : 10 : 8, weight ratio) at 180°C for the different reaction times without the cooling process, namely, 0, 1, 3, 6, and 10 h. Increasing the reaction times, the content of CuO (JCPD card no. 89–2529) and Cu_2O (JCPD card no. 77–0199) was gradually decreased, and the above intermediates were completely reduced to form Cu particles.

Figure 1(b) shows the XRD patterns of the different weight ratio of $CuCl_2{\cdot}2H_2O$ and the mixture of eutectic NaOH-KOH (the constant weight ratio of $CuCl_2{\cdot}2H_2O$ and PPG-400 is 1 : 8), i.e., 1 : 0, 1 : 1, 1 : 2.5, 1 : 5, and 1 : 10. The cubic CuCl (JCPD card no. 82–2114) can be obtained at 180°C for 10 h without eutectic NaOH-KOH. Increasing the weight of molten salt, the purity of the product is significantly enhanced. Consequently, Cu particles with little Cu_2O impurity are successfully synthesized by the reaction of $CuCl_2{\cdot}2H_2O$, eutectic NaOH–KOH and PPG-400 (1: 10: 8, weight ratio) at 180°C for 10 h.

TEM and FESEM studies of Cu products and CuCl intermediate reveal the different morphological features, as shown in Figure 2. Rod-like CuCl particles are successfully prepared because of the presence of nonionic surfactant polypropylene glycol (PPG-400), most of which have length up to about 100 nm with diameters ranging from 20 to 50 nm. The size of the copper particles is 400–500 nm as shown in Figure 2(b).

The reason of successful preparation of CuCl intermediate and Cu product by the one-pot reaction of $CuCl_2{\cdot}2H_2O$, eutectic NaOH–KOH and polyol at 180°C for 10 h is simple to understand.[11,23] The reaction equations of synthesis of Cu particles are shown in Figure 3. Firstly, the polyaldehydes are obtained by the intermolecular reaction of PPG-400, which possess complexation and reduction mechanism of different metal to prepare low valence state compound with various morphologies [Figure 3(a)]. Grayish CuCl particles are prepared by the reduction reaction of $CuCl_2{\cdot}2H_2O$ and polyaldehydes at 180°C for 10 h [Figure 3(e)]. Cu particles can be directly obtained by the one-pot reaction of $CuCl_2{\cdot}2H_2O$, eutectic NaOH-KOH and polyol at 180°C for 10 h [Figure 3(b–d)]. It is clear that Cu_2O intermediate can be quickly prepared under alkali condition. However, the speed of reducing Cu_2O to form Cu particles may be slow relatively.

Furthermore, the eutectic NaOH–KOH plays an important role in preparation of pure Cu particles. The molten salt can not only increase the solubility of reagent and intermediate at 180°C, but also enhance the reduction activity of polyaldehydes. CuO can be easily obtained by $CuCl_2{\cdot}2H_2O$ and eutectic NaOH–KOH at 180°C for 10 h. However, Cu cannot be directly synthesized by the reaction of CuO and PPG-400.

Figure 4 shows the mechanical properties of Cu/MWCNTs/ABS and MWCNTs/ABS composites with different content of Cu particles and MWCNTs as shown in Table I. It is clear that the ultimate tensile strength and tensile modulus of composites can be significantly improved by blending with Cu particles and MWCNTs. For example, upon incorporation of 7 wt % MWCNTs (S6 and S10), the ultimate tensile strength of the pure ABS is greatly improved by about 44 and 50%, and the elastic modulus is improved by about 21 and 31%. The mechanical properties of MWCNTs/ABS composites are slightly greater than Cu/MWCNTs/ABS composites because Cu particles probably influence the toughening effect. The possible toughening mechanism will be discussed later by FESEM observations.

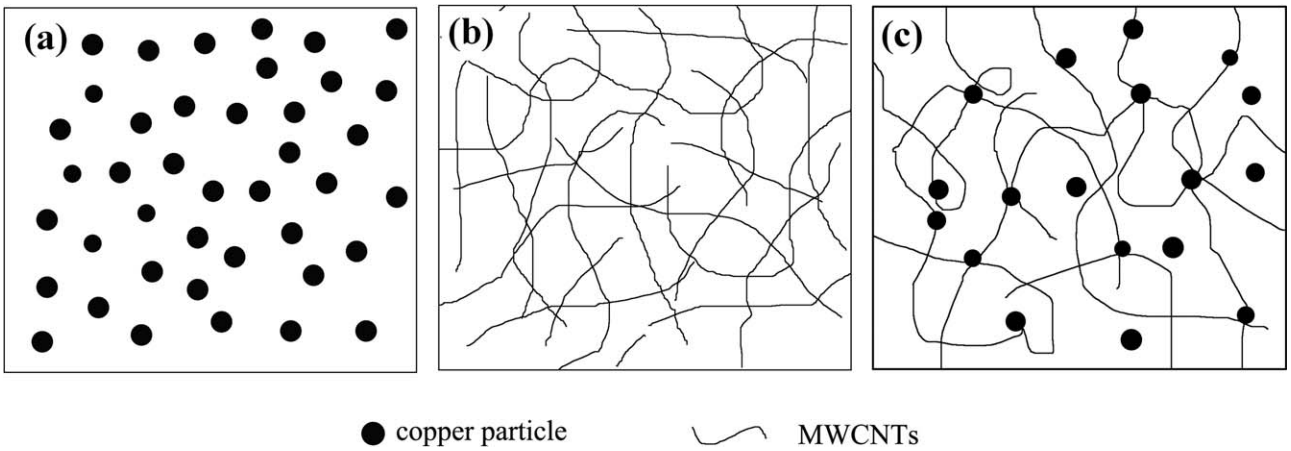

Figure 7. The sketch of the synergistic effect of Cu/MWCNTs/ABS composites.

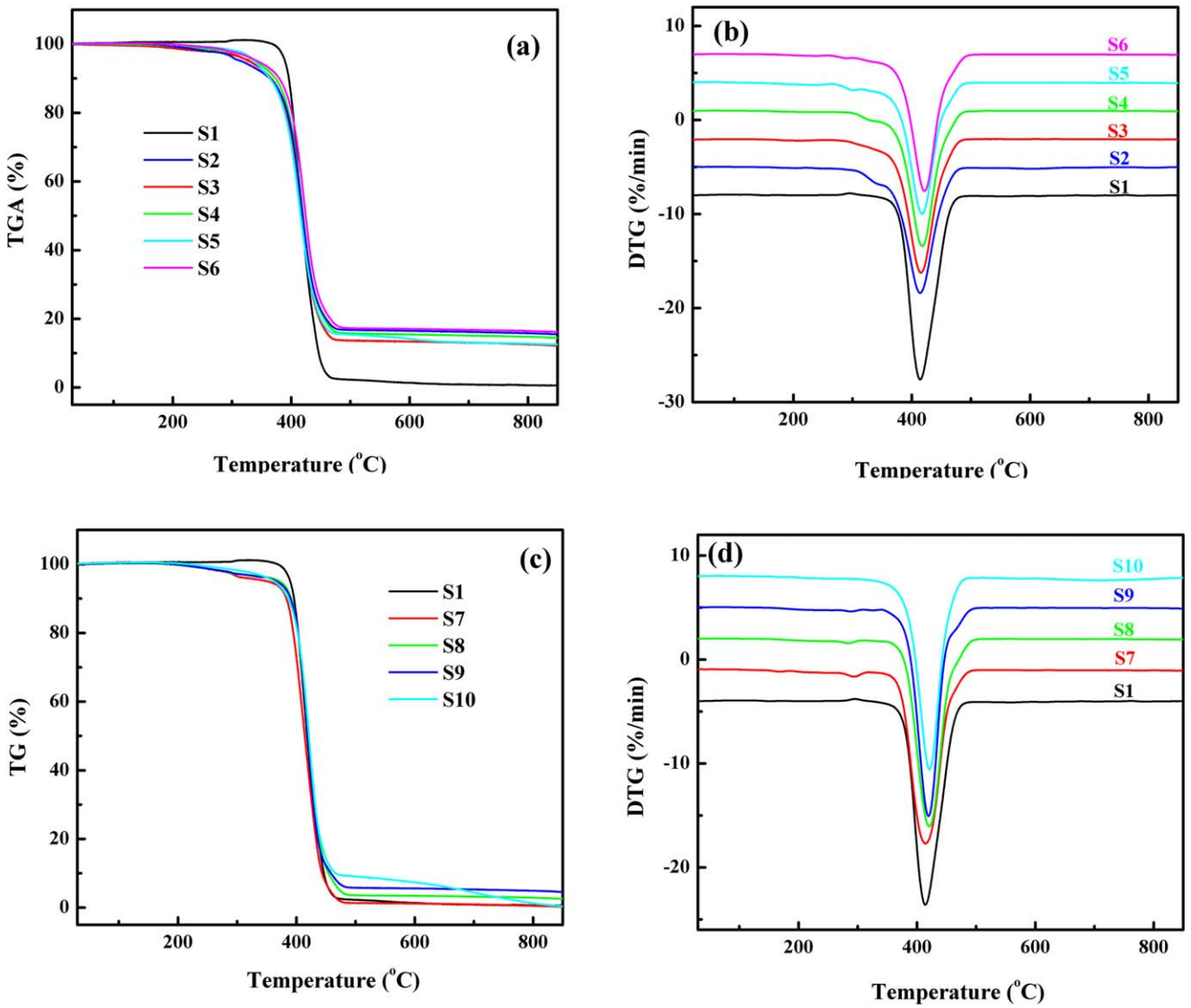

Figure 8. (a) TGA curves and (b) DTG curves of Cu/MWCNTs/ABS composites, (c) TGA curves and (d) DTG curves of MWCNTs/ABS composites under nitrogen atmosphere. [Color figure can be viewed in the online issue, which is available at wileyonlinelibrary.com.]

FESEM micrographs of fracture surfaces of the different samples of Cu/MWCNTs/ABS and MWCNTs/ABS composites are shown in Figure 5 to reveal the possible reinforcing mechanisms. The morphology of fracture surfaces of S2 is shown in Figure 5 (S2), which reveals that some voids are distributed within the structure in comparison with the S1 composite. The size of the voids is about 1μm that is obviously larger than Cu particles. It is significant that the fine compatibility of Cu/ABS composite and the dominant energy absorbing mechanism of the debonding of the Cu particles.[24]

After adding MWCNTs into the Cu/ABS blends, as shown in Figure 5 (S3–S6), ones can clearly see that the nanotubes (bright spots) are homogeneously dispersed in the ABS matrix without any visible agglomerates. With increasing the content of MWCNTs, more and more bright spots are found and they tend to overlap each other to form MWCNTs networks. At the same time, the fractured surface of the blends presents less concave holes, which illustrates most Cu particles fractured together with MWCNTs instead of being peeled off the Cu particles during the process of tensile measurement. Figure 5 (S7–S10) shows FESEM micrographs of fracture surfaces of MWCNTs/ABS composites without Cu particles. More careful observation shows that MWCNTs are all well-dispersed in the blends without any visible agglomerates, and it is also noted that the MWCNTs are anchored to the ABS firmly.

Figure 6 shows the electrical resistivity of Cu/MWCNTs/ABS and MWCNTs/ABS composites with the different content of MWCNTs. For samples with only Cu (S2), the electrical resistivity of Cu/ABS composites decreases slightly at the Cu content of 10 wt %. Nevertheless, addition of only a few amounts of MWCNTs leads to a dramatic decrease of electrical resistivity. Drop-offs in electrical resistivity are found in the case of Cu/MWCNTs/ABS and MWCNTs/ABS, which is obvious that electron activation for transition started for S5 and S9, respectively. However, the electrical resistivity of S5 is much lower than S9 with the same content of MWCNTs. This means that with the aid of very few amounts of Cu particles, much fewer MWCNTs is required to obtain the greater conductive composites. In other words, Cu and MWCNTs exhibit a synergistic effect in decreasing the electrical resistivity of Cu/MWCNTs/ABS blend. Therefore, electrical percolation threshold exists in the range of 3–5 wt % of the MWCNTs of the system of Cu/MWCNTs/ABS composites.

To give a more vivid description of the synergistic effect of Cu/MWCNTs/ABS composites, a sketch is drawn according to the above discussions in Figure 7. It is difficult to form the conductive pathway with little Cu particles which present the obvious distance of each other as shown in Figure 7(a). The electrical resistivity of Cu/MWCNTs/ABS composites was greater than MWCNTs/ABS composites without Cu particles, because Cu fillers can locate between MWCNTs chain segments provides a better charge transport in the conductive pathways as shown in Figure 7(b,c).

Figure 8 gives the thermogravimetric analysis (TGA) and derivative TGA (DTG) curves for the Cu/MWCNTs/ABS and MWCNTs/ABS composites under nitrogen atmosphere. The data for the maximum mass loss rate (v_{max}) and the temperature of the maximum mass loss rate (T_{max}) obtained from the DTG curves, are listed in Table I. The thermal decomposition of the pure ABS (S1) with maximum mass loss rate and the temperature of the maximum mass loss rate appear at 19.59 wt %/min and 414.4°C, respectively. Compared with the pure ABS, the initial decomposition temperatures and the residues of the composites containing Cu and MWCNTs are evidently improved. Although the initial decomposition temperature of the composites (S2–S10) is lower than S1, the maximum mass loss rate is decreased and the temperature of the maximum mass loss rate is increased, it further indicates that the chars effectively adhere to Cu and MWCNTs. The improved thermal stability under nitrogen conditions also confirms the synergistic role of the Cu and MWCNTs.

CONCLUSIONS

The polyol process was used successfully to reduce copper chloride to copper submicron particles. Then, the different system of Cu/MWCNTs/ABS and MWCNTs/ABS composites was successfully prepared and studied in mechanical, conductive, and thermal properties. Compared with pure ABS, the ultimate tensile strength and the elastic modulus of the sample S6 are greatly improved by about 44 and 21%, the maximum mass loss rate is decreased from 19.59 to 14.55 wt %/min and the temperature of the maximum mass loss rate is increased from 414.4 to 421.6°C. In addition, electrical percolation threshold exists in the range of 3–5 wt % of the MWCNTs of the system of Cu/MWCNTs/ABS composites. In other words, Cu and MWCNTs exhibit a synergistic effect in reinforcing mechanical, conductive, and thermal properties.

ACKNOWLEDGMENTS

Thanks to the Scientific Research Innovation Foundation of Jiangsu Province (No. CXZZ13_0894) and the National Natural Science Foundation of China (Grant No. 51403181).

REFERENCES

1. Jian, X.; Jiang, M.; Zhou, Z. W.; Zeng, Q.; Lu, J.; Wang, D. C.; Zhu, J. T.; Gou, J. H.; Wang, Y.; Hui, D.; Yang, M. L. *ACS Nano.* **2012**, *6*, 8611.
2. Khanna, P. K.; Gaikwad, S.; Adhyapak, P. V.; Singh, N.; Marimuthu, R. *Mater. Lett.* **2007**, *61*, 4711.
3. Lai, D. Z.; Liu, T.; Jiang, G. H.; Chen, W. X. *J. Appl. Polym. Sci.* **2013**, *128*, 1443.
4. Huang, Y.; Sarkar, D. K.; Chen, X. G. *Mater. Lett.* **2010**, *64*, 2722.
5. Ramyadevi, J.; Jeyasubramanian, K.; Marikani, A.; Rajakumar, G.; Rahuman, A. A. *Mater. Lett.* **2012**, *71*, 114.
6. Yan, C. L.; Xue, D. F. *Crystallogr. Growth Des.* **2008**, *8*, 1849.
7. Zhao, M. Q.; Sun, L.; Crooks, R. M. *J. Am. Chem. Soc.* **1998**, *120*, 4877.
8. Wu, S. H.; Chen, D. H. *J. Colloid Interface Sci.* **2004**, *273*, 165.
9. Vidyasagar, C. C.; Naik, Y. A.; Venkatesha, T. G.; Viswanatha, R. *Nano-Micro Lett.* **2012**, *4*, 73.

10. Chen, H. H.; Anbarasan, R.; Kuo, L. S.; Tsai, M. Y.; Chen, P. H.; Chiang, K. F. *Nano-Micro Lett.* **2010**, *2*, 101.
11. Chiang, T. H.; Tsai, M. H.; Syu, J. Y. *J. Inorg. Organomet. Polym.* **2013**, *23*, 712.
12. Sun, J. H.; Jing, Y.; Jia, Y. Z.; Tillard, M.; Belin, C. *Mater. Lett.* **2005**, *59*, 3933.
13. Lakshmi, K.; John, H.; Joseph, R.; Mathew, K. T.; George, K. E. *J. Appl. Polym. Sci.* **2012**, *124*, 5254.
14. Aneli, J. N.; Zaikov, G. E.; Khananashvili, L. M. *J. Appl. Polym. Sci.* **1999**, *74*, 601.
15. Xiong, Z. Y.; Wang, L.; Sun, Y.; Guo, Z. X.; Yu, J. *Polymer* **2013**, *54*, 447.
16. Chen, J.; Du, X. C.; Zhang, W. B.; Yang, J. H.; Zhang, N.; Huang, T.; Wang, Y. *Compos. Sci. Technol.* **2013**, *81*, 1.
17. Jung, J.; Kim, M.; Choi, J. K.; Park, D. W.; Shim, S. E. *Polymer* **2013**, *54*, 7071.
18. Maiti, S.; Suin, S.; Shrivastava, N. K.; Khatua, B. B. *J. Appl. Polym. Sci.* **2013**, *130*, 543.
19. Zhang, Y.; Liu, H.; Zhang, L.; Li, X. P.; Du, H. N.; Zhang, J. *J. Appl. Polym. Sci.* **2013**, *129*, 2744.
20. Nair, K. P.; Thomas, P.; Joseph, R. *Mater. Design.* **2012**, *41*, 23.
21. Al-Saleh, M. H.; Gelves, G. A.; Uttandaraman, S. *Mater. Design.* **2013**, *52*,128.
22. Sahoo, G. K.; Mazumder, R. *Ferroelectrics* **2010**, *402*, 193.
23. Fievet, F.; Lagier, J. P.; Figlarz, M. *MRS Bull.* **1989**, *14*, 29.
24. Ding, K. H.; Wang, G. L.; Zhang, M. *Mater. Des.* **2011**, *32*, 3986.